

LIS1 and NudE Induce a Persistent Dynein Force-Producing State

Richard J. McKenney,^{1,4} Michael Vershinin,^{2,4,6} Ambarish Kunwar,³ Richard B. Vallee,^{1,5,*} and Steven P. Gross^{2,5,*}

¹Department of Pathology and Cell Biology, Columbia University, New York, NY 10032, USA

²Department of Developmental and Cell Biology, University of California, Irvine, Irvine, CA 92697, USA

³Department of Neurobiology, Physiology & Behavior, University of California, Davis, Davis, CA 95616, USA

⁴These authors contributed equally to this work

⁵These authors contributed equally to this work

⁶Present address: Department of Physics, University of Utah, Salt Lake City, UT 84112, USA

*Correspondence: rv2025@columbia.edu (R.B.V.), sgross@uci.edu (S.P.G.)

DOI 10.1016/j.cell.2010.02.035

SUMMARY

Cytoplasmic dynein is responsible for many aspects of cellular and subcellular movement. LIS1, NudE, and NudEL are dynein interactors initially implicated in brain developmental disease but now known to be required in cell migration, nuclear, centrosomal, and microtubule transport, mitosis, and growth cone motility. Identification of a specific role for these proteins in cytoplasmic dynein motor regulation has remained elusive. We find that NudE stably recruits LIS1 to the dynein holoenzyme molecule, where LIS1 interacts with the motor domain during the pre-powerstroke state of the dynein crossbridge cycle. NudE abrogates dynein force production, whereas LIS1 alone or with NudE induces a persistent-force dynein state that improves ensemble function of multiple dyneins for transport under high-load conditions. These results likely explain the requirement for LIS1 and NudE in the transport of nuclei, centrosomes, chromosomes, and the microtubule cytoskeleton as well as the particular sensitivity of migrating neurons to reduced LIS1 expression.

INTRODUCTION

The major form of cytoplasmic dynein (dynein I; MAP1C) is involved in a wide range of cell movements, including vesicular and macromolecular transport, mitosis, and cell migration. The diversity of functions for this motor protein is matched by the complexity of its regulatory factors. LIS1 is a dynein-interacting protein encoded by the gene responsible for classical (type I) lissencephaly in humans (Reiner et al., 1993), a severe brain developmental disease. An ortholog of LIS1, *NudF*, was identified in a common “nuclear distribution” pathway with cytoplasmic dynein in *Aspergillus nidulans* (Xiang et al., 1995). An additional gene identified in the screen, *NudE*, has two mammalian counterparts, *Nde1* and *Ndel1* (protein names NudE and

NudEL) (Efimov and Morris, 2000; Feng et al., 2000; Niethammer et al., 2000; Sasaki et al., 2000).

LIS1 and NudE/NudEL are now understood to have additional, more general functions in the cytoplasmic dynein pathway, including nuclear and centrosomal transport in migrating neurons (Shu et al., 2004; Tsai et al., 2005; Tsai et al., 2007), centrosome positioning in migrating nonneuronal cells (Dujardin et al., 2003; Shen et al., 2008; Stehman et al., 2007), growth cone advance (Grabham et al., 2007), chromosome alignment, and mitotic spindle orientation (Faulkner et al., 2000; Liang et al., 2007; Siller et al., 2005; Stehman et al., 2007; Vergnolle and Taylor, 2007).

The specific roles of LIS1, NudE, and NudEL in cytoplasmic dynein regulation are poorly understood. LIS1 associates with mitotic kinetochores via cytoplasmic dynein, rather than the reverse (Coquelle et al., 2002; Tai et al., 2002), suggesting that LIS1 is not employed in dynein recruitment to these structures. In contrast, NudE and NudEL can recruit both dynein and LIS1 to centrosomes and kinetochores (Guo et al., 2006; Stehman et al., 2007; Vergnolle and Taylor, 2007). LIS1, NudE, and NudEL interact physically with each other (Feng et al., 2000; Niethammer et al., 2000; Sasaki et al., 2000; Tarricone et al., 2004) and with the cytoplasmic dynein motor and cargo-binding domains (Sasaki et al., 2000; Stehman et al., 2007; Tai et al., 2002) and have been reported to have limited effects on dynein enzymatic activity (Mesngon et al., 2006; Yamada et al., 2008). LIS1 has also been reported either to stimulate (Sapir et al., 1997) or to suppress microtubule assembly (Han et al., 2001) and to interfere with dynein-mediated microtubule gliding (Yamada et al., 2008), but its effects on dynein at the single-molecule level are unknown.

In the current study, we used biochemical and biophysical approaches to investigate whether and how LIS1 and NudE might affect dynein motor activity. We find that NudE recruits LIS1 to the dynein molecule, and that, surprisingly, LIS1 binds to the dynein motor domain at the prepowerstroke stage in its crossbridge cycle. Using single-molecule measurements we find that NudE inhibits dynein force production. LIS1 alone or with NudE converts dynein to a sustained-force state and markedly enhances ensemble motor function for high load transport. These data provide insight into the molecular basis for

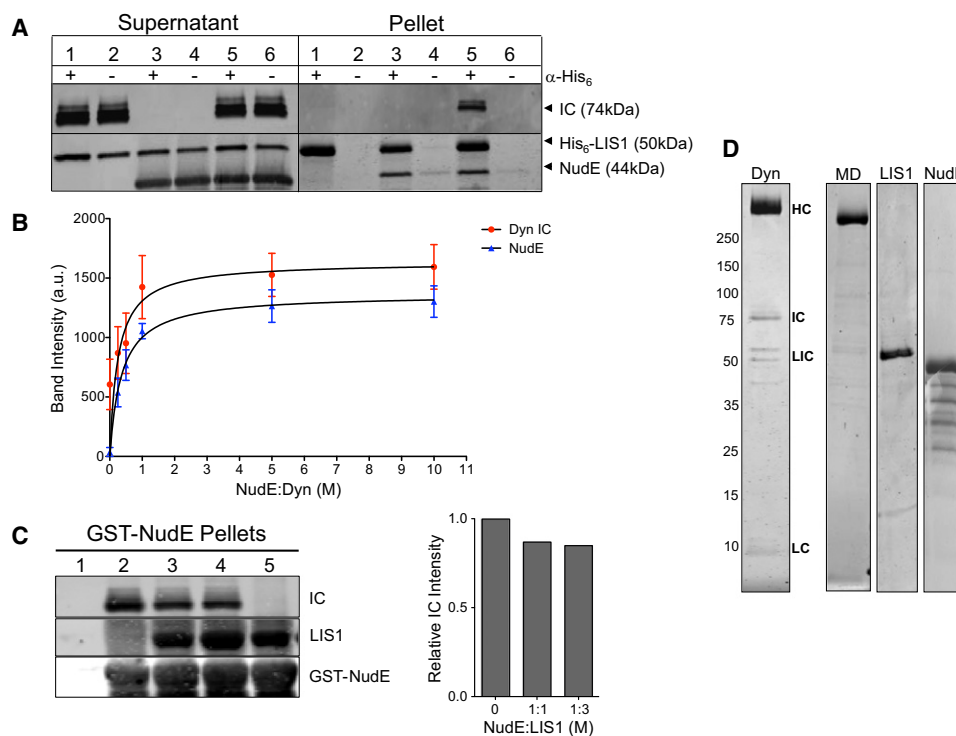


Figure 1. Dynein-NudE-LIS1 Interactions

(A) Recruitment of LIS1 to dynein by NudE. His₆-tagged LIS1 was immunoprecipitated with anti-His₆ antibody in the presence of purified brain dynein, NudE, or both. Immunoblotting shows no detectable coimmunoprecipitation of dynein (visualized by anti-intermediate chain [IC] antibody) with LIS1 (Pellet, lane 1) unless NudE is included (Pellet, lane 5).

(B) NudE concentration dependence of LIS1-dynein interaction. NudE was added in increasing amounts to a mixture of LIS1 and dynein, and the mixture was adsorbed to protein A beads coated with LIS1 antibodies. Quantitation of dynein (IC) and NudE pulled-down with LIS1 is shown. Dynein binding saturated at ~1:1 molar ratio with NudE. Mean of raw band intensity from four experiments is plotted in arbitrary units (a.u.) \pm standard deviation (SD).

(C) LIS1 and dynein do not compete for NudE. GST-NudE-coated beads were mixed with dynein either in the absence of LIS1 (lane 2) or the presence of 1- (lane 3) or 3-fold (lane 4) molar stoichiometry of LIS1:NudE. The added LIS1 did not substantially affect the amount of dynein that bound to NudE, confirming that NudE can bind both LIS1 and dynein simultaneously (see Figure 7A). No proteins bound to beads without NudE (lane 1) and LIS1 could bind to NudE in the absence of dynein (lane 5). Right, quantification of the relative amount of dynein IC in the absence and presence of added LIS1 protein.

(D) Coomassie brilliant blue-stained gels of purified cytoplasmic dynein complex and recombinant proteins used in this study. MD: Purified dynein motor domain. Dynein subunits: HC—heavy chain; IC—intermediate chain; LIC—light intermediate chain; LC—light chain. Bands below NudE represent fragments, as judged by immunoblotting with anti-NudE antibody.

See also Figure S1.

lissencephaly and the mechanism of action of LIS1, NudE, and NudEL in a broad range of biological functions.

RESULTS

Cooperative, Nucleotide-Dependent LIS1, NudE, and Dynein Interactions

To define more completely the interactions between dynein and LIS1 or NudE, we used recombinant LIS1 and NudE and purified cytoplasmic dynein from calf brain (Paschal et al., 1987) using a method that includes a deaffinity step to specifically deplete kinesin motors as potential contaminants. The purified dynein holoenzyme (Figure 1D) is a complex of two 532 kDa heavy chains, the C-terminal 2/3 of which corresponds to the motor domains. The N-terminal dynein tail domains mediate dimerization and interactions with intermediate, light intermediate, and light chains. To examine dynein motor domain interactions

specifically, we used a previously characterized 380 kDa baculovirus-expressed C-terminal dynein heavy chain fragment (Hook et al., 2005).

LIS1 coimmunoprecipitates with the cytoplasmic dynein holoenzyme complex (Faulkner et al., 2000; Smith et al., 2000) and with individual dynein subunits (Sasaki et al., 2000; Tai et al., 2002), but these interactions are relatively weak (Mesngon et al., 2006) (Figure 1A). Despite yeast two-hybrid and mammalian cell coexpression evidence for an interaction between LIS1 and the AAA1 ATPase portion of the dynein motor domain (Sasaki et al., 2000; Tai et al., 2002), we detect no cosedimentation of recombinant LIS1 with the purified 380 kDa baculovirus-expressed dynein motor domain (Figures 2A and 2B). To test whether this disparity could relate to changes in motor conformational states, we evaluated the effects of nucleotide and nucleotide analogs on the LIS1-motor domain interaction. We observed little or no interaction in the absence of nucleotide or

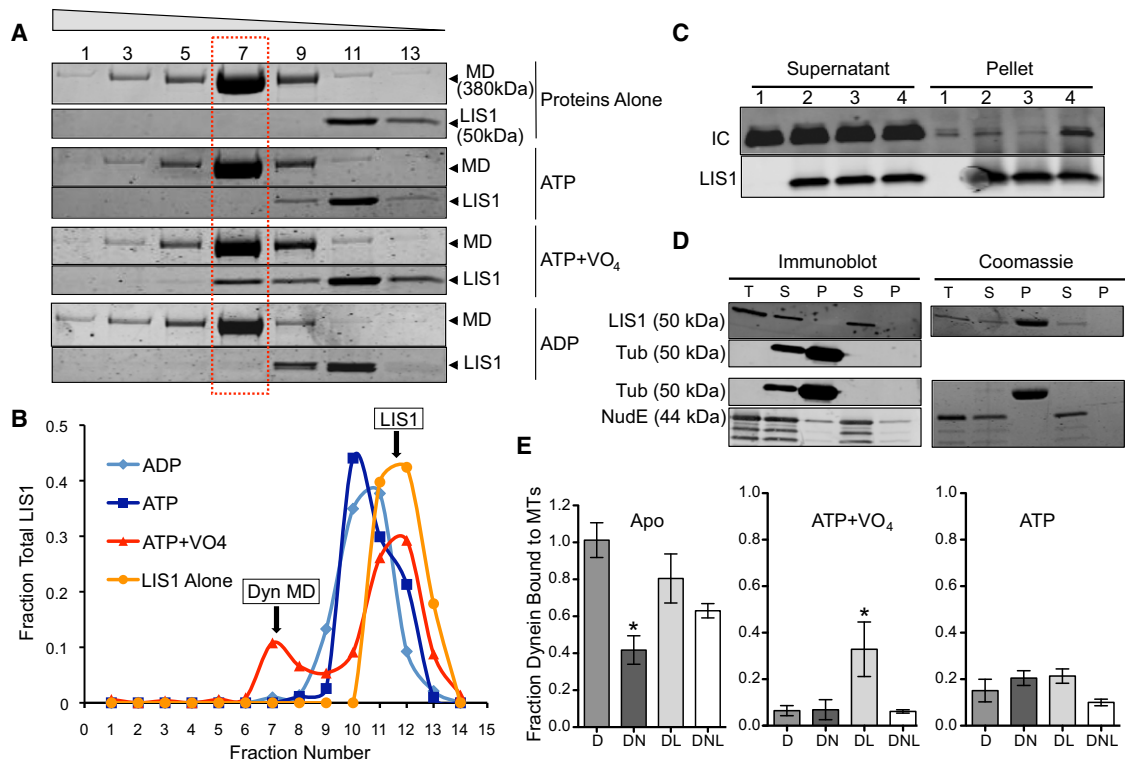


Figure 2. Effect of Nucleotides on Dynein-NudE-LIS1 Interactions

(A) Effect of nucleotides on LIS1 binding to dynein motor domain. Purified baculovirus-expressed dynein motor domain (MD) and LIS1 were incubated separately or together and sedimented through sucrose gradients containing the indicated nucleotides. Coomassie brilliant blue-stained gels show a fraction of LIS1 to cosediment with the purified dynein motor domain peak (dashed box) in the presence of ATP and VO₄ but not ATP alone or ADP. Sucrose concentration and fraction numbers are indicated at top.

(B) Quantitation of LIS1 distribution showing a major low *s* value peak for the free protein and, in the ATP+VO₄ condition, a smaller peak cosedimenting with the dynein motor domain.

(C) Effect of nucleotides on LIS1 binding to purified calf brain dynein. Dynein was incubated with beads alone (lane 1) or LIS1-coated beads in the absence of nucleotide (lane 2) or in the presence of ATP (lane 3) or ATP+VO₄ (lane 4). Dynein (IC) is enriched in the LIS1 pellet only in the ATP+VO₄ condition.

(D) LIS1 and NudE do not bind to microtubules. Purified LIS1 and NudE were sedimented in the presence or absence of microtubules. Total protein (T), supernatants (S) and pellets (P) are shown by immunoblotting and Coomassie blue staining. LIS1 is obscured by tubulin in the Coomassie blue-stained gel, but immunoblotting shows LIS1 not to sediment with microtubules. NudE also shows no evidence of microtubule cosedimentation.

(E) Effect of LIS1 and NudE on dynein binding to microtubules. Purified brain dynein was mixed with microtubules in the absence of nucleotide (Apo) or in the presence of ATP or ATP+VO₄, and the microtubules were sedimented. NudE strongly inhibited binding of dynein to microtubules in the apo state (DN; **p* = 0.0011, two-tailed *t* test), an effect partially rescued by LIS1 (DNL). Conversely, LIS1 increased dynein binding to microtubules in the ATP+VO₄ state by approximately 5-fold (DL; **p* = 0.0131, two-tailed *t* test). Error bars represent mean ± SD of three experiments.

in the presence of ATP, AMPPNP (not shown), or ADP but a clear interaction in the presence of ATP plus sodium vanadate (VO₄), as indicated by a shift in LIS1 to the dynein motor domain peak (molar ratio dynein motor:LIS1 dimer = 1.3; Figures 2A and 2B). A similar, nucleotide-dependent interaction is seen between LIS1 and the purified brain dynein (Figure 2C). ATP hydrolysis in the presence of VO₄ leads to a dynein-ADP-VO₄ dead-end complex, which is thought to mimic the prepower stroke transition state (Shimizu and Johnson, 1983), strikingly revealed by electron microscopy (Burgess et al., 2003). Our results suggest, therefore, that LIS1 interacts with the dynein motor domain at a specific, transient stage in its enzymatic cycle. The interaction site within the motor domain remains to be explored further but could involve AAA1 (Sasaki et al., 2000; Tai et al., 2002).

NudEL has been reported to interact with the dynein motor domain on the basis of yeast two-hybrid analysis (Sasaki et al., 2000). We detect no interaction between recombinant NudE and dynein motor domain under any nucleotide condition (Figure S1B available online) but have, instead, observed a clear interaction between NudE and the intact cytoplasmic dynein complex mediated through the intermediate and light chains located in the base of the dynein molecule (Stehman et al., 2007). NudE and NudEL bind through an unstructured C-terminal domain to dynein, and to LIS1 through a distinct N-terminal coiled-coil domain (Derewenda et al., 2007; Liang et al., 2004; Sasaki et al., 2000; Tarricone et al., 2004; Yan et al., 2003), leading us to speculate that NudE or NudEL might act to link LIS1 to dynein (Figure 7). Indeed, in the absence of nucleotide, the ability of LIS1 to pull down purified calf brain dynein was

completely dependent on addition of NudE (Figures 1A and 1B). The interaction showed a clear NudE concentration dependence and appeared to saturate at a molar stoichiometry of $\sim 1:1$ NudE:dynein (Figure 1B). LIS1 and dynein showed no evidence of competition for NudE binding (Figure 1C). Together, our results indicate that LIS1 alone interacts transiently with the dynein motor domain, but that NudE tethers LIS1 to dynein to form a more stable tripartite complex.

We also examined the effects of LIS1 and NudE on dynein-microtubule interactions. Alone, neither LIS1 nor NudE bound microtubules (Figure 2D). LIS1 had little effect on dynein-microtubule binding in the apo or ATP state (Figure 2E) but increased binding 5.1-fold in the presence of ADP-VO₄ (Figure 2E). This increase is intriguing because dynein binds weakly to microtubules in this condition (Imamura et al., 2007; Shimizu and Johnson, 1983). Thus, our data suggest that LIS1 increases the affinity of dynein for microtubules specifically during the prepowerstroke stage of the crossbridge cycle.

In contrast, NudE decreased dynein-microtubule binding by 60% in the absence of nucleotide, which corresponds to the strong binding (apo) state of the dynein mechanochemical cycle (Figure 2E). Little further effect on dynein-microtubule binding was observed in the presence of ATP or ATP plus VO₄ (Figure 2E).

LIS1 had no effect on basal or microtubule-stimulated dynein ATPase activity in our assays (Figure S1A), in contrast to one report (Mesngon et al., 2006) but consistent with another (Yamada et al., 2008). However, the microtubule-stimulated component of dynein ATPase activity was inhibited 50% by addition of NudE alone and by 72% with further addition of LIS1 (Figure S1A).

Effect of LIS1 on Dynein Behavior in Single-Molecule Assays

To determine the effects of LIS1 and NudE on the behavior of individual dynein molecules directly, we adsorbed dynein to carboxylated polystyrene beads and monitored transport and force production according to established methods (Gennerich et al., 2007; Mallik et al., 2004; Vershinin et al., 2008). Dynein was applied at dilutions at which $\leq 30\%$ of beads bound to microtubules (bead-binding fraction ≤ 0.3) to ensure predominantly single-motor events (Svoboda and Block, 1994). In the absence of applied force, dynein induced bead translocation at $\sim 1 \mu\text{m/s}$ (Figure 3), within the range of previous reports (King and Schroer, 2000; Mallik et al., 2005; Paschal and Vallee, 1987; Ross et al., 2006) but ~ 10 -fold faster than recombinant yeast cytoplasmic dynein (Reck-Peterson et al., 2006). Some bidirectional motion was observed, as previously reported (Gennerich et al., 2007; Mallik et al., 2005; Ross et al., 2006). Moderate levels of LIS1 did not affect processivity (Figure 3A), but net bead velocity was somewhat reduced due to increased bead pausing. Discrete pauses were infrequent at 1:1 LIS1:dynein but increased with LIS1 concentration (Figure 3C; note extreme example in Figure S3).

To test for effects of LIS1 on dynein force production, optical trapping was employed at single dynein molecule levels. The dynein beads showed clear evidence of force production, as previously described (Gennerich et al., 2007; Mallik et al., 2004; Reck-Peterson et al., 2006; Toba et al., 2006), with a stall force

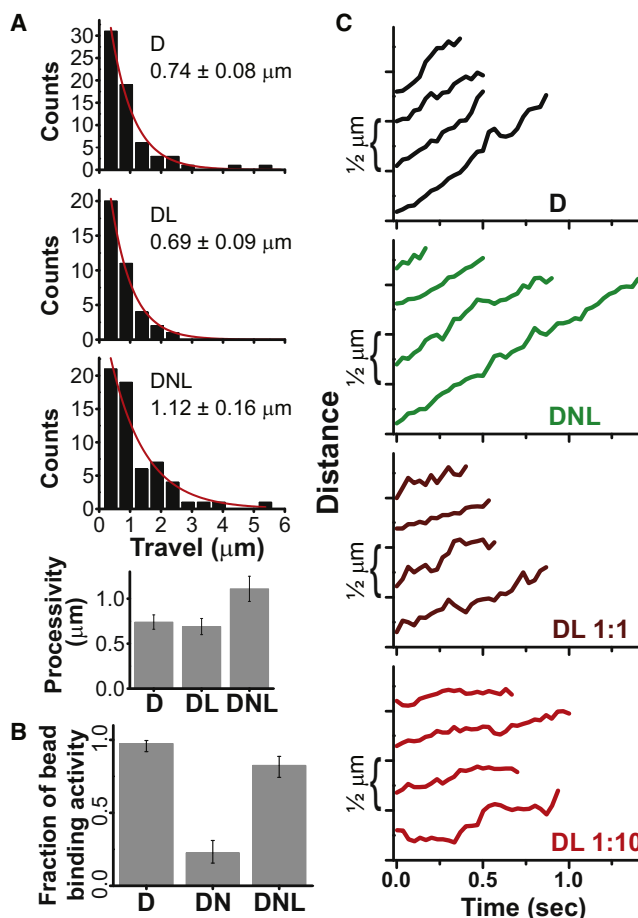


Figure 3. Effect of LIS1 and NudE on Dynein Motility

(A) Histogram of single dynein travel distances alone (D), in the presence of LIS1 (molar ratio of D:L = 1:2), and in the presence of both NudE and LIS1 (D:N:L = 1:9:10). Exponential decay fits are shown in red, and decay constant \pm standard error of the mean (SEM) is indicated in each case. A small percentage of beads had bidirectional motion of $2 \mu\text{m}$ or more in each direction, did not spontaneously detach from microtubules, and were excluded from analysis; such beads showed no force production capacity in either direction and were deemed to be diffusive rather than processive. D and DL processivity values are similar, whereas DNL processivity is clearly increased ($p < 0.03$).

(B) Microtubule-binding activity for D, DN, and DNL beads. We quantify the percentage of beads with visible binding and travel events, held close to a microtubule in a weak optical trap (See Experimental Procedures). NudE (molar ratio 1:9 D:N) potentially reduced microtubule-binding activity, an effect rescued by addition of LIS1 (D:N:L = 1:9:2). Neither LIS1 nor NudE produced a comparable inhibition of binding activity in similar experiments with kinesin motors (Figure S2B). Exact CI error bars are reported (see Supplemental Information).

(C) Individual traces of motor-driven movements along microtubules (D:L ratios indicated; D:N:L is as in A). D (black) and DNL (green) beads show robust motility whereas DL bead movements (dark and light red) are interrupted by pauses that result in a net slow-down of transport. The effect becomes more prominent as the LIS1 concentration increases. See Figure S3 for more extended and extreme examples of bead travel. For all experiments, dynein was first adsorbed to beads, followed as needed by NudE and then by LIS1.

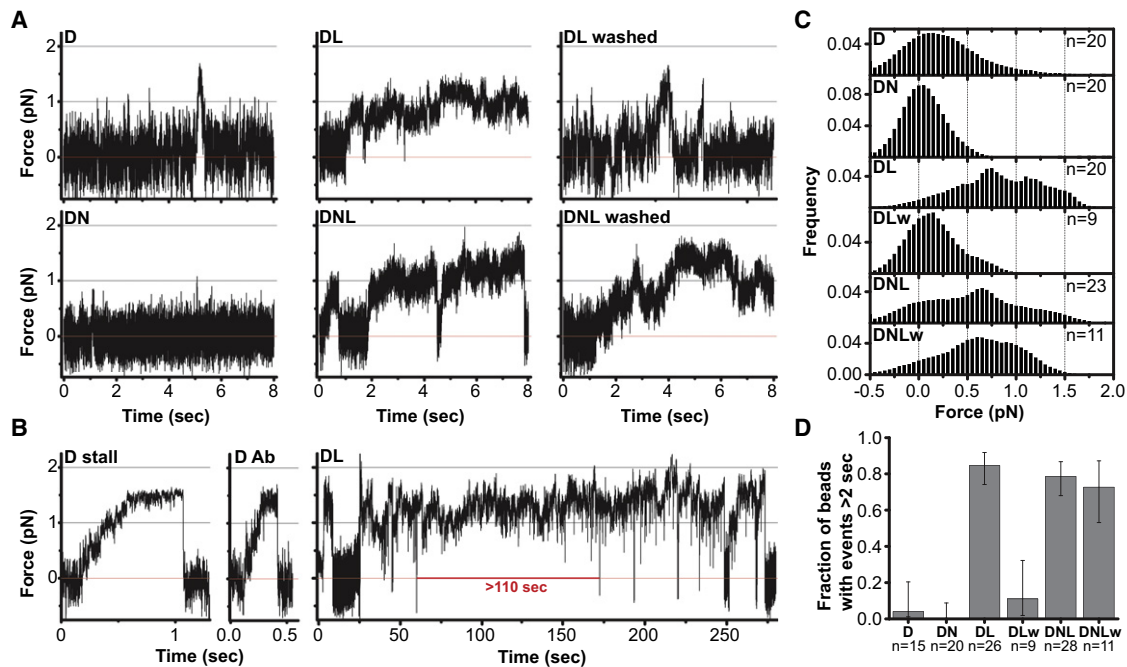


Figure 4. The Effect of NudE and LIS1 on Dynein Force Production

(A) Representative records of single-motor force production in an optical trap for beads with bound dynein (D); dynein + NudE (DN); dynein + LIS1 (DL); and dynein + NudE + LIS1 (DNL). Red line marks center of optical trap. Dynein beads (D) typically detach before the motor can stall, but short (~ 0.5 s) stalls occasionally occur (see B). DN beads (1:9 D:N) show almost no motion. However, DL and DNL beads (1:2 D:L and 1:9:2 D:N:L) exhibit dramatically longer force production events, some of which continue beyond the period shown (and see panel B). Similar behavior under load was also observed at higher amounts of LIS1 (1:10 D:L) in DL and DNL assays (see Figure S4). The prolonged dynein stalls induced by LIS1 were eliminated by washing the beads (see Experimental Procedures) in the DL assay (DL washed) but not the DNL assay (DNL washed). These observations support our biochemical results indicating that NudE retains LIS1 in a complex with dynein (Figures 1A and 1B).

(B) Representative stalls for dynein adsorbed to beads nonspecifically (D stall) or through anti-dynein IC monoclonal antibody (D Ab) illustrate maximal force production for single dynein motors. (DL) An extremely long (~ 110 s) event (entire tracing is shown) demonstrating dramatic prolongation of dynein force production by LIS1.

(C) Distribution of forces attained during prominent bead-microtubule binding events sampled in a 4 s window and summed from multiple bead assays ($n = 9\text{--}23$ as indicated). DN shows minimal bead displacement almost symmetrically distributed around the trap center, indicating that bead motion is predominantly due to thermal noise. D alone exhibits a shift to higher forces. The shift is dramatically greater for DL and DNL, indicating higher average force production. Notably, this effect was retained when DNL beads were washed to remove excess proteins from solution (DNLw) but abolished when DL beads were similarly washed (DLw). This suggests that DNL association is stable but the DL one is not.

(D) The fraction of beads exhibiting long force production events (>2 s) is dramatically increased in the presence of LIS1. The effect is again abolished in DL-washed (DLw) but not in DNL-washed (DNLw) assays. Exact CI error bars are reported (see Supplemental Information). See also Figure S4.

of 1.0–1.5 pN (Mallik et al., 2004; Schroeder et al., 2008; Figures 4A and 4B). Comparable values were obtained with dynein bound directly to beads or through an anti-dynein intermediate chain antibody (1.4 ± 0.2 pN, $n = 11$; Figure 4B, “D Ab”) and for chicken and mouse cytoplasmic dynein (1.3–1.4 pN, J. Xu and K. Ori-McKenney, personal communication). Another vertebrate dynein preparation has been reported with a higher stall force when adsorbed nonspecifically to protein A-coated beads, but with differences in several additional properties (Toba et al., 2006). Yeast cytoplasmic dynein has also been reported to have a higher stall force (Reck-Peterson et al., 2006), but its 10-fold slower transport rate and C-terminally truncated motor domains suggest a phylogenetic basis for its differences from mammalian cytoplasmic dynein.

As reported (Mallik et al., 2004), clean dynein stalling events could be detected in the optical trap (Figure 4B, panel “D stall”;

Figure S4, top), but, more typically, dynein detached before reaching its full stall load (Figure 4A, panel “D”). The maximum duration of dynein stalls was ~ 2 s, as reported (Mallik et al., 2004). In marked contrast, addition of LIS1 induced periods of dramatically sustained load-bearing events (Figure 4). These persistent “stall-like events” lasted from several seconds to >100 s in the longest case. Periods of sequential stall-like events with only transient interruptions were also common and lasted up to 250 s (Figure 4B, “DL,” additional examples Figure S4). Analysis of combined tracings from multiple beads revealed that, in the presence of LIS1, dynein beads spent much more time at higher average forces (Figure 4C, panels D versus DL).

These effects reflect LIS1-induced alteration of dynein behavior based on several considerations. LIS1 showed no microtubule binding on its own (see above, Figure 2D), nor did LIS1-coated beads bind microtubules (Figure S1). The LIS1

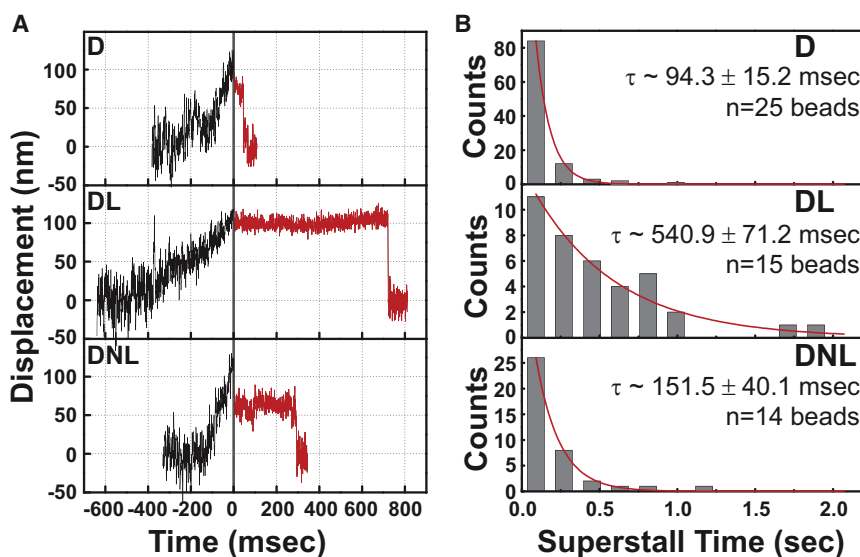


Figure 5. LIS1 Enhances Dynein-Microtubule Interaction under Load

(A) Beads driven by single dynein motors were allowed to move along microtubules in a weak optical trap (black traces). At 100 nm bead displacement from the trap center, laser power was automatically increased ($T = 0$, solid vertical line), subjecting dynein to a load of ~ 2 pN, significantly greater than the dynein stall force (“superstall” conditions). Subsequent bead positions are shown as red lines and demonstrate prolonged persistence of DL bead (1:10 D:L) on microtubule and less so of DNL (1:9:10 D:N:L) bead.

(B) Analysis of multiple superstall traces as in (A) revealed that average detachment times in both DL and DNL assays were significantly increased relative to D alone. Exponential decay constant \pm SEM is shown in each subpanel.

effect on dynein could be eliminated by preincubation of the his-tagged LIS1 with Ni^{2+} -NTA beads (data not shown) and specifically retained by NudE in bead-washing experiments (see below). Finally, LIS1 showed no biochemical interaction with kinesin, nor did it affect kinesin-mediated bead transport or the duration of kinesin stalls (Figure S2).

Effects of NudE and NudE Plus LIS1 on Dynein Behavior in Single-Molecule Assays

In contrast to LIS1, and consistent with its effect on dynein microtubule binding (Figure 2E), NudE reduced the frequency of microtubule-binding events by dynein beads (Figure 3B). Bead travel in the presence of NudE was typically below the level of noise-driven fluctuations (~ 25 – 40 nm; Figure 4A, “DN”). Because of the minimal bead binding in the presence of NudE, the optical trap was needed to hold beads in proximity to microtubules. The overall effect of NudE was a dramatic reduction in dynein-mediated force production (Figure 4C, “DN”). As for LIS1, and consistent with our biochemical analysis (Figure 2D), beads coated with NudE alone showed no microtubule-binding activity (Figure S1 and Figure 2D). Furthermore, NudE showed no binding to kinesin and had little effect on the ability of kinesin beads to bind microtubules or produce force (Figure S2).

To test the combined effects of LIS1 and NudE, we exposed beads to dynein, followed by NudE and LIS1 (see Experimental Procedures). LIS1 rescued the dramatic inhibition of bead-microtubule interactions observed with NudE alone (Figure 3B). Conversely, NudE completely eliminated LIS1-induced bead pausing (Figure 3C), as indicated by visual inspection of bead traces and by restoration of average bead velocity ($D = 1.05 \pm 0.12$; DL at 1:10 = 0.23 ± 0.04 ; DNL at 1:10:10 = 1.04 ± 0.06). In addition, LIS1 plus NudE significantly increased dynein bead processivity relative to dynein-coated beads alone (Figures 3A and 3C). Most significantly, NudE and LIS1 together dramatically increased the duration of dynein stall-like events (Figure 4 and Figure S4), but with maximal force levels unchanged.

Our biochemical analysis indicated that NudE mediates the interaction between dynein and LIS1. To test whether NudE recruits LIS1 to dynein in the bead assay, we adsorbed dynein at single-molecule concentrations, followed by LIS1 alone or LIS1 with NudE. We then removed excess proteins by centrifugation and resuspension of the beads in motility buffer alone. For beads exposed to dynein and LIS1, the effect of LIS1 was markedly reduced by washing. For beads exposed to dynein, LIS1, and NudE and then washed, clear preservation of sustained force events was observed (Figure 4, DL versus DL washed; and DL washed versus DNL washed). We conclude that NudE, indeed, stabilizes the LIS1-dynein interaction in these assays.

Direct Analysis of LIS1-Modulated Dynein Detachment from Microtubules under Load

Pull-off experiments (Evans, 2001) assay the strength of protein-protein interactions directly with high temporal and spatial resolution and were used to measure dynein’s affinity for microtubules with or without LIS1 and NudE. When trapped beads had moved ~ 100 nm from the trap center, laser intensity was doubled to exceed the dynein stall force (“superforce”). Typically, after very brief pauses, dynein beads detached from the microtubule and returned rapidly toward the trap center with a $t_{1/2} = 94.2$ ms (Figures 5A and 5B). In the presence of LIS1, dynein beads remained attached up to 1–2 s ($t_{1/2} = 540.9$ ms; Figures 5A and 5B, panels “DL”). LIS1 and NudE combined also increased the duration of binding relative to dynein alone, though less substantially. Thus, LIS1 allows dynein to remain bound longer under load, indicating that LIS1 increases the effective strength of the dynein-microtubule interaction.

Effects of NudE and LIS1 on Dynein Behavior in Multiple-Motor Assays

How multiple motors function together to achieve active transport is only partially understood. To explore how LIS1 and NudE affect the behavior of multiple dynein motors, we conducted

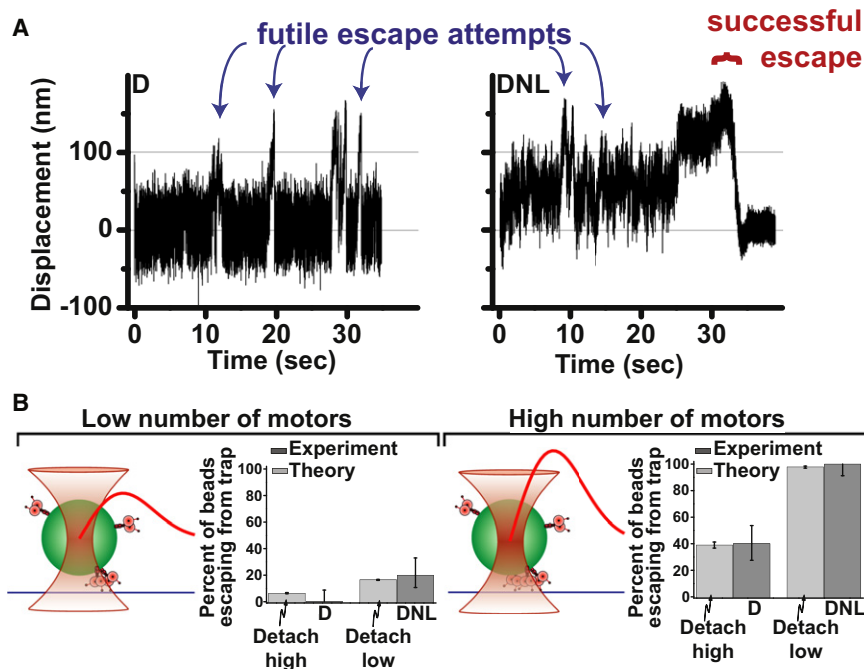


Figure 6. LIS1 and NudE Enhance Multiple-Motor Function

To test the effect of NudE and LIS1 on multiple dynein motors, beads were incubated with concentrations of dynein above those used for single-molecule experiments.

(A) Force records from individual beads exposed to dynein (D) or the same amount of dynein followed by NudE and LIS1 (DNL). High force events can be observed (blue arrows), as can bead escapes from trap confinement (red bracket).

(B) Quantification of trap escape. The fraction of high force events resulting in escape was scored for D versus DNL at low (left) and high (right) concentrations of applied dynein (dark gray bars, $n = 20$ in each case). Maximum trap force was estimated at 1.8 pN and 3.7 pN for these two assays, respectively (therefore, synergistic activity of ≥ 2 and ≥ 3 motors was required for a successful escape event to occur in these two assays, respectively). The frequency of trap escapes was clearly increased in DNL versus D alone. Theoretical modeling (light gray bars) conservatively assuming a 50% change of time to detachment for each dynein motor (*cf* Figure 5B) is predicted to be sufficient to account for the observed difference between D and DNL escape frequencies (see

[Extended Experimental Procedures](#)). Schematic

diagram of the experiment (left of each histogram): the bead (green) with motors attached to its surface (rose) is held near a microtubule (blue) by an optical trap (hyperboloid shape). Trap strength (red curve) rises approximately linearly as the distance from trap center grows, then saturates and finally decays to zero. Exact CI error bars are reported (see [Extended Experimental Procedures](#)). See also [Figure S5](#).

“trap escape” assays using beads incubated with increased concentrations of dynein. Force production was monitored for two different force/motor-number combinations, using either a 1.8 pN escape force (requiring two motors to escape, [Figure 6B](#), left) or a 3.7 pN escape optical trap (sufficient to prevent two but not three dynein motors from escaping, [Figure 6B](#), right). The addition of LIS1 and NudE caused a significant increase in the number of beads able to escape from the optical trap along microtubules ([Figures 6A](#) and [6B](#)), consistent with a dramatic improvement in multiple-motor performance.

To determine whether the large improvement in multiple-motor performance could be explained by the LIS1-induced decreased detachment rate under load, we modeled single dynein motor activity using a Monte-Carlo approach used for kinesin ([Kunwar et al., 2008](#)) but reflecting unique features of dynein motility (most notably non-negligible back-stepping probability even under zero load). Importantly, modeling was highly constrained by experimental data, especially microtubule dissociation rate and stall force (this study) and back-stepping rate ([Mallik et al., 2005](#)). Dynein motility modeled in this way was similar to the experimentally observed records ([Figure S5A](#)). We then expanded the single dynein model to simulate two or more motors functioning together to match each of the two experimental conditions ([Figure 6](#)) for motor ensemble performance under load. Thus, motor number was adjusted in the simulation until the correct proportion of dynein-only beads escaped from the trap ([Figure 6B](#), bars labeled “detach high”). The simulations for the dynein-NudE-LIS1 case were then performed identically, except for the change in individual motor

detachment rate under load ([Figure 5](#)). This theoretical change in single-molecule properties indeed yielded a predicted change in ensemble motor function, so that the resulting frequency of high-force motility events was very comparable to the trap escape frequency we observed experimentally due to addition of NudE and LIS1 ([Figure 6B](#), bars labeled “detach low,” [Figure S5B](#)), with no additional adjustments or free parameters required. Thus, the modeling suggests that the improved multiple-motor behavior observed experimentally can be entirely explained by the measured cofactor-induced changes in single-molecule function. Technical details of the theoretical modeling are provided in the [Experimental Procedures](#) and the [Extended Experimental Procedures](#).

DISCUSSION

LIS1, cytoplasmic dynein, NudE, and NudEL have long been known to function in a common genetic pathway. The mechanistic implications of the interactions among these proteins have remained a major question in the field of developmental neuroscience, motor protein research, and cell biology. NudE and NudEL have been implicated in some aspects of dynein recruitment to subcellular sites, but this has not been the case for LIS1, and its functions as well as how its activity may be modulated by NudE and NudEL have remained largely unknown.

LIS1 is essential for neuronal migration, based on the altered distribution of neurons in the lissencephalic brain ([Dobyns, 1987](#); [Hirotsune et al., 1998](#); [Reiner et al., 1993](#)) and direct imaging of migrating neurons in fixed ([Shu et al., 2004](#)) and live

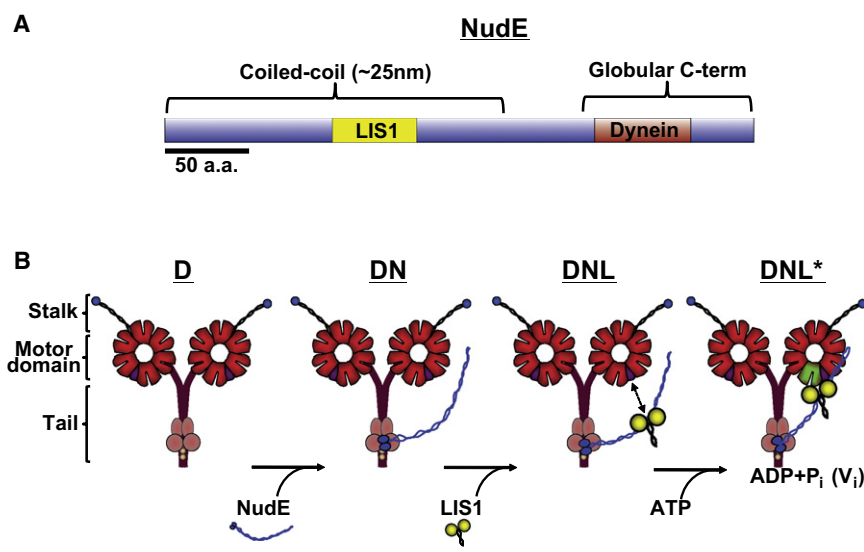


Figure 7. Diagrammatic Representation of Dynein-LIS1-NudE Interactions and Functional Consequences

(A) Bar diagram of NudE shows coiled-coil and unstructured C-terminal domains and known LIS1- and dynein-binding regions (see text for details).

(B) Proposed assembly intermediates in dynein-NudE-LIS1 complex. Known binding of NudE to dynein intermediate and light chains (Stehman et al., 2007) predicts an association of the NudE C terminus with the base of the dynein molecule, with its coiled-coil domain postulated to protrude as shown. The calculated distance between the NudE-dynein site and the known LIS1-binding site in the middle of the NudE coiled-coil α -helical tail (Derewenda et al., 2007) is proposed here to be sufficient to allow NudE to position LIS1 near the dynein motor domains. LIS1 is shown unbound to the dynein motor domain as we observe under most conditions but is proposed to bind specifically in the ADP-VO₄ prepowerstroke state (Figure 2).

embryonic brain tissue (Tsai et al., 2005). No other dynein-related effects have been reported to be altered in humans with LIS1 mutations or in mouse models. LIS1 dominant-negative cDNAs had potent effects on cell migration and division, but not on other dynein functions such as Golgi, endosome, and lysosome positioning (Faulkner et al., 2000, though see Smith et al., 2000). LIS1 may, thus, contribute to a subset of cytoplasmic dynein functions, but the nature of its specific role has been obscure. Here we identify LIS1 and NudE as regulators of dynein force production, the first such proteins implicated in this role. How this behavior relates to the biological functions of LIS1 is discussed below.

LIS1-NudE-Dynein Complex

Despite prior evidence for a LIS1-dynein motor domain interaction (Sasaki et al., 2000; Tai et al., 2002), it must be very weak or transient in view of the lack of binding we typically observe between the purified components (Figure 1D). We find, however, that NudE can mediate LIS1 binding to the dynein complex in an efficient, saturable, and apparently stoichiometric manner (Figures 1A, 1B, and 7). Consistent with this conclusion, NudE retained LIS1 on dynein beads washed to remove free protein (Figures 4A, 4C, and 4D).

Our data provide evidence for a triple complex of LIS1, NudE, and cytoplasmic dynein, with a potential structural arrangement as shown in Figure 7B. NudE and NudEL interact via an unstructured C-terminal domain with the dynein intermediate and light chains (Stehman et al., 2007) at the base of the dynein molecule (Figure 7B). LIS1, in contrast, interacts within the N-terminal coiled-coil region of NudE and NudEL (amino acids 103–153 and 102–152, respectively) (Derewenda et al., 2007; Sasaki et al., 2000) (Figure 7B). The LIS1 site, therefore, can be estimated to lie approximately 15 nm from the C terminus of NudE. As depicted in Figure 7B, association of NudE with the intermediate and light chains at the base of the dynein molecule could, therefore, place LIS1 close to the motor domains. Whether NudE and LIS1 are oriented in this manner is unknown. However, our biochemical and biophysical evidence that LIS1

linked to dynein through NudE remains capable of altering dynein motor function makes this an appealing speculation.

We suggest, therefore, that NudE and NudEL serve in communication between the dynein tail and motor domains. Nonmuscle myosin II isoforms, myosin V, and some kinesins each exhibit such a mechanism, but through direct intramolecular interactions between tail and motor domains (Dietrich et al., 2008; Kremontsov et al., 2004; Scholey et al., 1980; Stock et al., 1999; Wang et al., 2004). Such a feature is as yet unknown for cytoplasmic dynein. Our results suggest that NudE and/or NudEL could play such a role, though as the first extramolecular factors with such a function.

Effects of LIS1 and NudE on Dynein Motor Activity

We find LIS1 and NudE each to have dramatic effect on cytoplasmic dynein motor activity in our single-molecule assays. LIS1 prolonged dynein force-producing events, often for substantial periods of time. LIS1 likely acts at a precise stage in the dynein crossbridge cycle, as it bound to the dynein motor domain only in the presence of ATP plus VO₄ (Figure 2A), which arrests dynein at the prepowerstroke state. LIS1 also caused a 5-fold enhancement of dynein binding to microtubules under these conditions (Figure 2E), suggesting a specific increase in microtubule affinity in the prepowerstroke stage. Single-molecule superforce experiments (Figure 5) showed a decreased rate of dynein dissociation from microtubules under load, consistent with increased affinity (Gebhardt et al., 2006; Veigel et al., 2005). Together, our results reveal that LIS1 prolongs the interaction of dynein with microtubules, specifically during the prepowerstroke and possibly the powerstroke states. A similar transition state-specific interaction involving the bacterial enhancer-binding protein (EBP), another member of the AAA+ protein family, was recently reported (Chen et al., 2007), suggesting that transition state interactions may be an evolutionarily conserved mechanism in this extended protein superfamily.

NudE affected dynein behavior in a manner opposite from LIS1, but apparently at a different stage of the dynein crossbridge cycle, corresponding to the apo state. We observed no

binding of NudE to the dynein motor domain under any nucleotide condition (Figure S1B), in contrast to LIS1. However, NudE strongly decreased the ability of the purified brain dynein complex to bind to microtubules, and, in bead assays, single dynein-microtubule interactions were almost eliminated. Whether this potent NudE inhibition results from steric hindrance of the motor-microtubule interaction or more direct regulation of motor activity is uncertain. We do not confirm a previously reported weak interaction between NudEL and fragments of the dynein motor domain (Sasaki et al., 2000). This may be a result of the use of the complete motor domain in the current study, which we find to be physically and enzymatically very well behaved (Hook et al., 2005).

The combination of LIS1, dynein, and NudE produces what appears to be a streamlined molecular machine converted to function in sustained force production. The LIS1-induced pauses observed in freely moving beads are eliminated by the addition of NudE, and dynein processivity is increased, while prolongation of force-producing events persists. Furthermore, the concentration of LIS1 required for this effect appears to be greatly reduced, as the ability to induce prolonged force events persists following bead washing (Figures 4A and 4C). We hypothesize that these results reflect retention of LIS1 to dynein in the presence of NudE. In addition, we hypothesize that LIS1 is stereospecifically positioned by NudE for greater efficiency of dynein force regulation (Figure 7B).

We observed clear inhibition of microtubule-stimulated dynein ATPase activity by NudE alone and NudE plus LIS1 (Figure S1A), though we saw little effect of LIS1 alone. This result may simply reflect the preferential effect of LIS1 on dynein under load. It is also possible that dynein ATP hydrolysis persists during the stalled state, either from activity at the principal ATPase site, AAA1, or at the subsidiary sites (Kon et al., 2004). ATPase and microtubule-binding activity can be uncoupled in dynein stalk mutants (Kon et al., 2009), and it is conceivable that LIS1 could contribute to comparable effects. An earlier study also found little effect of LIS1 on dynein ATPase activity (Yamada et al., 2008), though another study found a modest ~40% stimulation (Mesngon et al., 2006). Further research will be needed to clarify what effects LIS1 may have on the complex dynein ATPase cycle.

Biological Implications

Our data have important biological implications. LIS1 is required for cytoplasmic dynein activities that appear to involve very high load, including transport of, or tension on, nuclei, chromosomes, and even the entire microtubule cytoskeleton (Grabham et al., 2007; Tsai et al., 2007). Nuclei, in particular, show signs of extreme distortion as they attempt to advance within migrating neurons against great resistance (Tsai et al., 2007). This resistance is overcome by LIS1 and dynein in control cells, but it is blocked by LIS1 or dynein RNAi (Tsai et al., 2007). By conferring on dynein the ability to resist release from microtubules under load, we envision that LIS1 permits the summation of individual dynein forces, resulting in greatly increased average force production. This is consistent with theoretical studies indicating that force-detachment kinetics affect ensemble motor function (Kunwar et al., 2008). Nuclear oscillatory movements

in *S. pombe* have been estimated to require ~50 dyneins (Vogel et al., 2009), many more than the 3–5 molecules reported for small membranous organelles (Shubeita et al., 2008; Soppina et al., 2009). Our test for LIS1-NudE stimulation of multimotor transport showed a dramatic increase in the ability to escape from an optical trap under high force conditions. These results reveal that, although individual dynein molecules are stalled under load in the presence of LIS1 and NudE, additional dynein-LIS1-NudE complexes strongly enhance the ability to move along microtubules under opposing loads. In silico modeling yielded virtually identical results (Figure 6B and Figure S5). We believe our results, therefore, explain the role of LIS1 in nuclear movement and likely in several additional cellular functions, including transport of large arrays of microtubules in radially migrating neurons and other cell types, mitotic spindle orientation, and aspects of chromosome movement. In contrast, we have found that small vesicular dynein cargoes showed no change in subcellular distribution in cells expressing LIS1 dominant-negative cDNA (Faulkner et al., 2000), and dynein-transported virus particles showed no detectable sensitivity to LIS1 inhibition (Bremner et al., 2009). Whether LIS1, nonetheless, could have some role in low load functions remains to be investigated more fully.

NudE and NudEL have been found to recruit dynein to kinetochores (Liang et al., 2007; Stehman et al., 2007; Vergnolle and Taylor, 2007), centrosomes (Guo et al., 2006), and possibly other structures. Therefore, we propose that these proteins target dynein and LIS1 to specific subcellular sites and, together with LIS1, control dynein force production as required. NudE and NudEL may have the additional function of silencing dynein at these sites until LIS1 is available, as suggested by the effects of NudE on single dynein molecules in the current assays.

EXPERIMENTAL PROCEDURES

Protein Purification

Bovine or rat brain cytoplasmic dynein, baculovirus-expressed dynein motor domain, and recombinant NudE were purified as described (Hook et al., 2005; Paschal et al., 1987; Stehman et al., 2007), except that the GST tag was removed from the NudE by PreScission protease cleavage (GE Biosciences). African green monkey LIS1 (Faulkner et al., 2000) was cloned into the Bac-N-Blue baculovirus system (Invitrogen) with an N-terminal His₆-tag and expressed according to the manufacturer's protocols. Recombinant kinesin (K560, Addgene- Cambridge, MA, USA) was expressed and purified using standard procedures.

Immunoprecipitations

Immunoprecipitation was performed using streptavidin beads (Invitrogen) incubated with a biotinylated monoclonal anti-His₆ antibody (QIAGEN) and then incubated with His₆-tagged LIS1 for 1 hr on ice. The beads were then mixed with NudE and/or dynein at 4°C for 1 hr in Tris-KCl buffer. Beads were then washed five times with buffer and samples were processed for western blot analysis using a LI-COR Odyssey imaging system.

Microtubule Binding

To assay effects of LIS1 and NudE on dynein microtubule binding, the proteins were mixed together at a 1:10 (Dyn:LIS1/NudE) ratio and incubated with 1 mg/ml final concentration of taxol-stabilized microtubules (Cytoskeleton, Inc.) and indicated nucleotides for 10 min at 37°C. ATP concentration was 10 mM with or without equimolar VO₄.

Bead Assays

Bead assays, including force measurements, and video recording and analysis of bead motion were performed essentially as previously described (Mallik et al., 2004; Vershinin et al., 2007) (for small exceptions, see [Extended Experimental Procedures](#)). Protein adsorption on beads was done via sequential incubations (10 min at room temperature) with motors, blocking agent (5.5 mg/ml casein), and dynein cofactors (LIS1 and NudE). Cofactors were removed by centrifugation in the “washed” assays and were left in solution in the “unwashed” assays. For data in [Figure 4B](#) (D Ab), the antibody was first nonspecifically adsorbed on beads followed by casein blocking and incubation with dynein (buffer exchanged at each step).

Superstall Experiments

Beads driven by a single dynein motor were subjected to ~ 2 pN of force (superstall condition) via a rapid change in optical trap stiffness. The duration of a superstall event was identified as the subsequent time for bead position to return to trap center.

Multiple-Motor Escape Experiments

Beads incubated with identical amounts of dynein in the presence or absence of NudE and LIS1 (parallel assays) were tested for ability to escape a trap of fixed stiffness. The fraction of escaped D and DNL beads was determined for two different dynein concentrations (and thus different mean number of engaged motors). Trap stiffness was different for each motor concentration.

Detailed methods can be found in the [Extended Experimental Procedures](#).

SUPPLEMENTAL INFORMATION

Supplemental Information includes [Extended Experimental Procedures](#) and five figures and can be found with this article online at [doi:10.1016/j.cell.2010.02.035](https://doi.org/10.1016/j.cell.2010.02.035).

ACKNOWLEDGMENTS

We acknowledge Drs. Jing Xu, Silvia Cermelli, and Peter Hook for helpful discussions and Shahnaz Kemal, Kassandra Ori-McKenney, and Z. Shu for technical help. This work was supported by grants GM47434 and HD40182 to R.B.V. and grants 1R01GM070676 and GM079156 to S.P.G. A.K. was supported by grant GM068952.

Received: May 18, 2009

Revised: December 18, 2009

Accepted: February 18, 2010

Published: April 15, 2010

REFERENCES

- Bremner, K.H., Scherer, J., Yi, J., Vershinin, M., Gross, S.P., and Vallee, R.B. (2009). Adenovirus transport via direct interaction of cytoplasmic dynein with the viral capsid hexon subunit. *Cell Host Microbe* 6, 523–535.
- Burgess, S.A., Walker, M.L., Sakakibara, H., Knight, P.J., and Oiwa, K. (2003). Dynein structure and power stroke. *Nature* 421, 715–718.
- Chen, B., Doucleff, M., Wemmer, D.E., De Carlo, S., Huang, H.H., Nogales, E., Hoover, T.R., Kondrashkina, E., Guo, L., and Nixon, B.T. (2007). ATP ground- and transition states of bacterial enhancer binding AAA+ ATPases support complex formation with their target protein, sigma54. *Structure* 15, 429–440.
- Coquelle, F.M., Caspi, M., Cordelieres, F.P., Dompierre, J.P., Dujardin, D.L., Koifman, C., Martin, P., Hoogenraad, C.C., Akhmanova, A., Galjart, N., et al. (2002). LIS1, CLIP-170's key to the dynein/dynactin pathway. *Mol. Cell Biol.* 22, 3089–3102.
- Derewenda, U., Tarricone, C., Choi, W.C., Cooper, D.R., Lukasik, S., Perrina, F., Tripathy, A., Kim, M.H., Cafiso, D.S., Musacchio, A., and Derewenda, Z.S. (2007). The structure of the coiled-coil domain of Ndel1 and the basis of its interaction with Lis1, the causal protein of Miller-Dieker lissencephaly. *Structure* 15, 1467–1481.
- Dietrich, K.A., Sindelar, C.V., Brewer, P.D., Downing, K.H., Cremona, C.R., and Rice, S.E. (2008). The kinesin-1 motor protein is regulated by a direct interaction of its head and tail. *Proc. Natl. Acad. Sci. USA* 105, 8938–8943.
- Dobyns, W.B. (1987). Developmental aspects of lissencephaly and the lissencephaly syndromes. *Birth Defects* 23, 225–241.
- Dujardin, D.L., Barnhart, L.E., Stehman, S.A., Gomes, E.R., Gundersen, G.G., and Vallee, R.B. (2003). A role for cytoplasmic dynein and LIS1 in directed cell movement. *J. Cell Biol.* 163, 1205–1211.
- Efimov, V.P., and Morris, N.R. (2000). The LIS1-related NUDF protein of *Aspergillus nidulans* interacts with the coiled-coil domain of the NUDE/RO11 protein. *J. Cell Biol.* 150, 681–688.
- Evans, E. (2001). Probing the relation between force–lifetime–and chemistry in single molecular bonds. *Annu. Rev. Biophys. Biomol. Struct.* 30, 105–128.
- Faulkner, N.E., Dujardin, D.L., Tai, C.Y., Vaughan, K.T., O'Connell, C.B., Wang, Y., and Vallee, R.B. (2000). A role for the lissencephaly gene LIS1 in mitosis and cytoplasmic dynein function. *Nat. Cell Biol.* 2, 784–791.
- Feng, Y., Olson, E.C., Stukenberg, P.T., Flanagan, L.A., Kirschner, M.W., and Walsh, C.A. (2000). LIS1 regulates CNS lamination by interacting with mNudE, a central component of the centrosome. *Neuron* 28, 665–679.
- Gebhardt, J.C., Clemen, A.E., Jaud, J., and Rief, M. (2006). Myosin-V is a mechanical ratchet. *Proc. Natl. Acad. Sci. USA* 103, 8680–8685.
- Gennerich, A., Carter, A.P., Reck-Peterson, S.L., and Vale, R.D. (2007). Force-induced bidirectional stepping of cytoplasmic dynein. *Cell* 131, 952–965.
- Grabham, P.W., Seale, G.E., Bennecib, M., Goldberg, D.J., and Vallee, R.B. (2007). Cytoplasmic dynein and LIS1 are required for microtubule advance during growth cone remodeling and fast axonal outgrowth. *J. Neurosci.* 27, 5823–5834.
- Guo, J., Yang, Z., Song, W., Chen, Q., Wang, F., Zhang, Q., and Zhu, X. (2006). Nudel contributes to microtubule anchoring at the mother centriole and is involved in both dynein-dependent and -independent centrosomal protein assembly. *Mol. Biol. Cell* 17, 680–689.
- Han, G., Liu, B., Zhang, J., Zuo, W., Morris, N.R., and Xiang, X. (2001). The *Aspergillus* cytoplasmic dynein heavy chain and NUDF localize to microtubule ends and affect microtubule dynamics. *Curr. Biol.* 11, 719–724.
- Hirotsune, S., Fleck, M.W., Gambello, M.J., Bix, G.J., Chen, A., Clark, G.D., Ledbetter, D.H., McBain, C.J., and Wynshaw-Boris, A. (1998). Graded reduction of *Pafah1b1* (*Lis1*) activity results in neuronal migration defects and early embryonic lethality. *Nat. Genet.* 19, 333–339.
- Hook, P., Mikami, A., Shafer, B., Chait, B.T., Rosenfeld, S.S., and Vallee, R.B. (2005). Long range allosteric control of cytoplasmic dynein ATPase activity by the stalk and C-terminal domains. *J. Biol. Chem.* 280, 33045–33054.
- Imamura, K., Kon, T., Ohkura, R., and Sutoh, K. (2007). The coordination of cyclic microtubule association/dissociation and tail swing of cytoplasmic dynein. *Proc. Natl. Acad. Sci. USA* 104, 16134–16139.
- King, S.J., and Schroer, T.A. (2000). Dynactin increases the processivity of the cytoplasmic dynein motor. *Nat. Cell Biol.* 2, 20–24.
- Kon, T., Imamura, K., Roberts, A.J., Ohkura, R., Knight, P.J., Gibbons, I.R., Burgess, S.A., and Sutoh, K. (2009). Helix sliding in the stalk coiled coil of dynein couples ATPase and microtubule binding. *Nat. Struct. Mol. Biol.* 16, 325–333.
- Kon, T., Nishiura, M., Ohkura, R., Toyoshima, Y.Y., and Sutoh, K. (2004). Distinct functions of nucleotide-binding/hydrolysis sites in the four AAA modules of cytoplasmic dynein. *Biochemistry* 43, 11266–11274.
- Krementsov, D.N., Krementsova, E.B., and Trybus, K.M. (2004). Myosin V: regulation by calcium, calmodulin, and the tail domain. *J. Cell Biol.* 164, 877–886.
- Kunwar, A., Vershinin, M., Xu, J., and Gross, S.P. (2008). Stepping, strain gating, and an unexpected force-velocity curve for multiple-motor-based transport. *Curr. Biol.* 18, 1173–1183.
- Liang, Y., Yu, W., Li, Y., Yang, Z., Yan, X., Huang, Q., and Zhu, X. (2004). Nudel functions in membrane traffic mainly through association with Lis1 and cytoplasmic dynein. *J. Cell Biol.* 164, 557–566.

- Liang, Y., Yu, W., Li, Y., Yu, L., Zhang, Q., Wang, F., Yang, Z., Du, J., Huang, Q., Yao, X., and Zhu, X. (2007). Nudel modulates kinetochore association and function of cytoplasmic dynein in M phase. *Mol. Biol. Cell* 18, 2656–2666.
- Mallik, R., Carter, B.C., Lex, S.A., King, S.J., and Gross, S.P. (2004). Cytoplasmic dynein functions as a gear in response to load. *Nature* 427, 649–652.
- Mallik, R., Petrov, D., Lex, S.A., King, S.J., and Gross, S.P. (2005). Building complexity: an in vitro study of cytoplasmic dynein with in vivo implications. *Curr. Biol.* 15, 2075–2085.
- Mesngon, M.T., Tarricone, C., Hebbar, S., Guillotte, A.M., Schmitt, E.W., Lanier, L., Musacchio, A., King, S.J., and Smith, D.S. (2006). Regulation of cytoplasmic dynein ATPase by Lis1. *J. Neurosci.* 26, 2132–2139.
- Niethammer, M., Smith, D.S., Ayala, R., Peng, J., Ko, J., Lee, M.S., Morabito, M., and Tsai, L.H. (2000). NUDEL is a novel Cdk5 substrate that associates with LIS1 and cytoplasmic dynein. *Neuron* 28, 697–711.
- Paschal, B.M., and Vallee, R.B. (1987). Retrograde transport by the microtubule associated protein MAP 1C. *Nature* 330, 181–183.
- Paschal, B.M., Shpetner, H.S., and Vallee, R.B. (1987). MAP 1C is a microtubule-activated ATPase which translocates microtubules *in vitro* and has dynein-like properties. *J. Cell Biol.* 105, 1273–1282.
- Reck-Peterson, S.L., Yildiz, A., Carter, A.P., Gennerich, A., Zhang, N., and Vale, R.D. (2006). Single-molecule analysis of Dynein processivity and stepping behavior. *Cell* 126, 335–348.
- Reiner, O., Carrozzo, R., Shen, Y., Wehnert, M., Faustinella, F., Dobyns, W.B., Caskey, C.T., and Ledbetter, D.H. (1993). Isolation of a Miller-Dieker lissencephaly gene containing G protein β -subunit-like repeats. *Nature* 364, 717–721.
- Ross, J.L., Wallace, K., Shuman, H., Goldman, Y.E., and Holzbaur, E.L. (2006). Processive bidirectional motion of dynein-dynactin complexes in vitro. *Nat. Cell Biol.* 8, 562–570.
- Sapir, T., Elbaum, M., and Reiner, O. (1997). Reduction of microtubule catastrophe events by LIS1, platelet-activating factor acetylhydrolase subunit. *EMBO J.* 16, 6977–6984.
- Sasaki, S., Shionoya, A., Ishida, M., Gambello, M.J., Yingling, J., Wynshaw-Boris, A., and Hirotsune, S. (2000). A LIS1/NUDEL/cytoplasmic dynein heavy chain complex in the developing and adult nervous system. *Neuron* 28, 681–696.
- Scholey, J.M., Taylor, K.A., and Kendrick-Jones, J. (1980). Regulation of non-muscle myosin assembly by calmodulin-dependent light chain kinase. *Nature* 287, 233–235.
- Schroeder, H.W., Shuman, H., Holzbaur, E.L., and Goldman, Y.F. (2008). Cargo switching at actin-microtubule intersections: a case for strength in numbers. *Mol. Biol. Cell* 19 (suppl.), 325/B269.
- Shen, Y., Li, N., Wu, S., Zhou, Y., Shan, Y., Zhang, Q., Ding, C., Yuan, Q., Zhao, F., Zeng, R., and Zhu, X. (2008). Nudel binds Cdc42GAP to modulate Cdc42 activity at the leading edge of migrating cells. *Dev. Cell* 14, 342–353.
- Shimizu, T., and Johnson, K.A. (1983). Kinetic evidence for multiple dynein ATPase sites. *J. Biol. Chem.* 258, 13841–13846.
- Shu, T., Ayala, R., Nguyen, M.D., Xie, Z., Gleeson, J.G., and Tsai, L.H. (2004). Ndel1 operates in a common pathway with LIS1 and cytoplasmic dynein to regulate cortical neuronal positioning. *Neuron* 44, 263–277.
- Shubeita, G.T., Tran, S.L., Xu, J., Vershini, M., Cermelli, S., Cotton, S.L., Welte, M.A., and Gross, S.P. (2008). Consequences of motor copy number on the intracellular transport of kinesin-1-driven lipid droplets. *Cell* 135, 1098–1107.
- Siller, K.H., Serr, M., Steward, R., Hays, T.S., and Doe, C.Q. (2005). Live imaging of *Drosophila* brain neuroblasts reveals a role for Lis1/dynactin in spindle assembly and mitotic checkpoint control. *Mol. Biol. Cell* 16, 5127–5140.
- Smith, D.S., Niethammer, M., Ayala, R., Zhou, Y., Gambello, M.J., Wynshaw-Boris, A., and Tsai, L.H. (2000). Regulation of cytoplasmic dynein behaviour and microtubule organization by mammalian Lis1. *Nat. Cell Biol.* 2, 767–775.
- Soppina, V., Rai, A.K., Ramaiya, A.J., Barak, P., and Mallik, R. (2009). Tug-of-war between dissimilar teams of microtubule motors regulates transport and fission of endosomes. *Proc. Natl. Acad. Sci. USA* 106, 19381–19386.
- Stehman, S.A., Chen, Y., McKenney, R.J., and Vallee, R.B. (2007). NudE and NudEL are required for mitotic progression and are involved in dynein recruitment to kinetochores. *J. Cell Biol.* 178, 583–594.
- Stock, M.F., Guerrero, J., Cobb, B., Eggers, C.T., Huang, T.G., Li, X., and Hackney, D.D. (1999). Formation of the compact conformation of kinesin requires a COOH-terminal heavy chain domain and inhibits microtubule-stimulated ATPase activity. *J. Biol. Chem.* 274, 14617–14623.
- Svoboda, K., and Block, S.M. (1994). Force and velocity measured for single kinesin molecules. *Cell* 77, 773–784.
- Tai, C.Y., Dujardin, D.L., Faulkner, N.E., and Vallee, R.B. (2002). Role of dynein, dynactin, and CLIP-170 interactions in LIS1 kinetochore function. *J. Cell Biol.* 156, 959–968.
- Tarricone, C., Perrina, F., Monzani, S., Massimiliano, L., Kim, M.H., Derewenda, Z.S., Knapp, S., Tsai, L.H., and Musacchio, A. (2004). Coupling PAF signaling to dynein regulation: Structure of LIS1 in complex with PAF-acetylhydrolase. *Neuron* 44, 809–821.
- Toba, S., Watanabe, T.M., Yamaguchi-Okimoto, L., Toyoshima, Y.Y., and Higuchi, H. (2006). Overlapping hand-over-hand mechanism of single molecular motility of cytoplasmic dynein. *Proc. Natl. Acad. Sci. USA* 103, 5741–5745.
- Tsai, J.W., Chen, Y., Kriegstein, A.R., and Vallee, R.B. (2005). LIS1 RNA interference blocks neural stem cell division, morphogenesis, and motility at multiple stages. *J. Cell Biol.* 170, 935–945.
- Tsai, J.W., Bremner, K.H., and Vallee, R.B. (2007). Dual subcellular roles for LIS1 and dynein in radial neuronal migration in live brain tissue. *Nat. Neurosci.* 10, 970–979.
- Veigel, C., Schmitz, S., Wang, F., and Sellers, J.R. (2005). Load-dependent kinetics of myosin-V can explain its high processivity. *Nat. Cell Biol.* 7, 861–869.
- Vergnolle, M.A., and Taylor, S.S. (2007). Cenp-F links kinetochores to Ndel1/Nde1/Lis1/dynein microtubule motor complexes. *Curr. Biol.* 17, 1173–1179.
- Vershini, M., Carter, B.C., Razafsky, D.S., King, S.J., and Gross, S.P. (2007). Multiple-motor based transport and its regulation by Tau. *Proc. Natl. Acad. Sci. USA* 104, 87–92.
- Vershini, M., Xu, J., Razafsky, D.S., King, S.J., and Gross, S.P. (2008). Tuning microtubule-based transport through filamentous MAPs: the problem of dynein. *Traffic* 9, 882–892.
- Vogel, S.K., Pavin, N., Maghelli, N., Julicher, F., and Tolic-Norrelykke, I.M. (2009). Self-organization of dynein motors generates meiotic nuclear oscillations. *PLoS Biol.* 7, e1000087.
- Wang, F., Thirumurugan, K., Stafford, W.F., Hammer, J.A., 3rd, Knight, P.J., and Sellers, J.R. (2004). Regulated conformation of myosin V. *J. Biol. Chem.* 279, 2333–2336.
- Xiang, X., Osmani, A.H., Osmani, S.A., Xin, M., and Morris, N.R. (1995). NudF, a nuclear migration gene in *Aspergillus nidulans*, is similar to the human LIS-1 gene required for neuronal migration. *Mol. Biol. Cell* 6, 297–310.
- Yamada, M., Toba, S., Yoshida, Y., Haratani, K., Mori, D., Yano, Y., Mimori-Kiyosue, Y., Nakamura, T., Itoh, K., Fushiki, S., et al. (2008). LIS1 and NDEL1 coordinate the plus-end-directed transport of cytoplasmic dynein. *EMBO J.* 27, 2471–2483.
- Yan, X., Li, F., Liang, Y., Shen, Y., Zhao, X., Huang, Q., and Zhu, X. (2003). Human Nudel and NudE as regulators of cytoplasmic dynein in poleward protein transport along the mitotic spindle. *Mol. Cell Biol.* 23, 1239–1250.